In Situ S K-Edge X-ray Absorption Spectroscopy for Understanding and Developing SO$_x$ Storage Catalysts

Hendrik Dathe, Andreas Jentys,* and Johannes A. Lercher[†]

Department of Chemistry, Technische Universität München, Lichtenbergstrasse 4, D-85747 Garching, Germany

Received: August 4, 2005; In Final Form: September 12, 2005

In situ S K-edge XANES experiments were carried out on second-generation SO$_x$ trapping materials under oxidizing and reducing conditions. The experiments clearly show that the strong release of SO$_2$ under rich conditions at plug flow conditions is caused by the facilitated reduction of sulfite species on Pt. In the absence of Pt the sulfite species were stable under reducing conditions, while maintaining a similar total SO$_2$ uptake capacity. Thus, SO$_x$ trapping materials without a noble metal are a clearly better option. The enhancing effect on the SO$_x$ storage process of water present in the gas mixture is attributed to the formation of a higher sulfate fraction in the samples. The application of the in situ S K-edge XANES technique clearly reveals new information and insights on the behavior of the sulfur in the trapping process compared to that from the ex situ measurements and is therefore essential for designing new SO$_x$ trapping materials.

1. Introduction

The combination of more efficient diesel engines and the tighter Euro IV emission standards for NO$_x$ require the introduction of new exhaust gas treatment technologies for NO$_x$. One of the most promising approaches for diesel passenger cars is the NO$_x$ storage−reduction (NO$_x$-SR) concept.[1,2] During a (long) period in which the exhaust gas is rich in oxygen (lean fuel conditions), NO is catalytically oxidized to NO$_2$ and stored in the form of nitrates. During short periods an excess of fuel is introduced (fuel-rich conditions), and the stored nitrates are catalytically reduced to nitrogen. The successful application of this technique in the automotive industry depends on solving the (complete) deactivation of the catalyst in the presence of SO$_x$ in the exhaust gas formed by the combustion of sulfur compounds in the fuel. During the oxygen-rich period the NO$_x$ trap generally acts as an oxidation catalyst, which leads to the formation of SO$_3$ and the subsequent formation of sulfates on the NO$_x$ storage material, typically consisting of base oxide materials (e.g., barium oxide). The sulfates formed are thermodynamically more stable than nitrates under reducing conditions (lean mode) and, therefore, lead to a permanent deactivation of the material for NO$_x$ storage.[3,4] A possible concept, facilitated by the low levels of sulfur in diesel and gasoline fuels (at present 10 ppm or less), is the use of disposable or ex situ regenerable sulfur traps for on-site removal of sulfur from emissions prior to contact with the NO$_x$-SR catalyst. The materials proposed for SO$_x$ trapping in exhaust emission control contain typically an oxidation component (e.g., a noble metal) to convert the SO$_2$ to SO$_3$ and a sulfur storage component (usually oxides of alkaline and earth alkaline metals) supported on α-Al$_2$O$_3$, Ce$_2$O$_3$, and ZrO$_2$.[5,6] However, limitations of the SO$_x$ uptake rate and the applicable SO$_x$ storage capacity limit the immediate application of such materials in the exhaust gas treatment of lean burn engines. For enhancing the performance of SO$_x$ trap materials a deeper insight into the sulfur storage process with
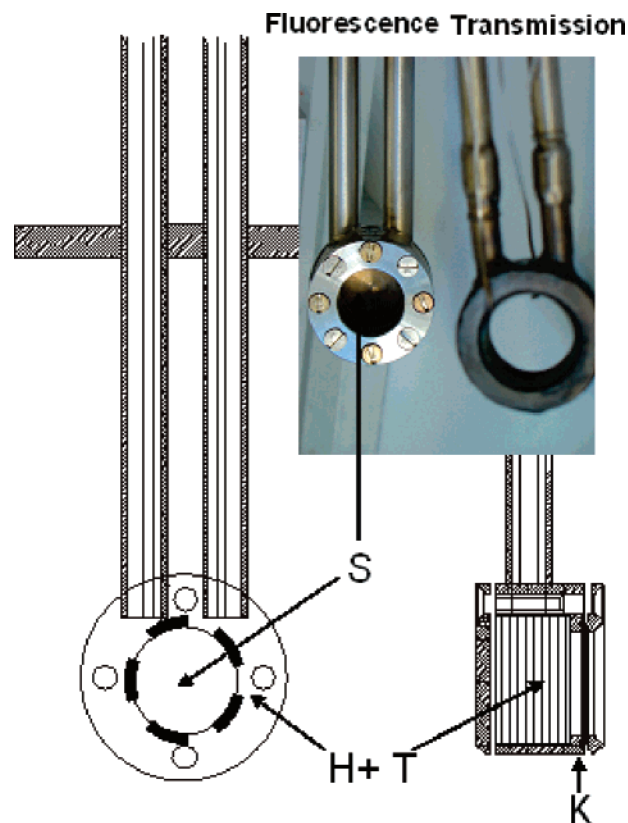

Figure 1. Experimental setup for measuring in situ time-resolved XANES at the S K-edge (H = heating; T = thermocouple; S = sample; K = 7.5 μm Kapton).

respect to the formation of the surface and bulk sulfur species, especially under cycling (lean/rich) conditions, is necessary.

Various techniques such as IR, Raman, or XPS give information about the state of sulfur present on the sample; however, strongly overlapping bands of bulk and surface sulfates formed (infrared spectroscopy) or the requirement of ultrahigh vacuum (X-ray photoelectron spectroscopy) limits most methods for in

* Corresponding author.
[†] Phone: +49 89 289 13540. Fax: +49 89 289 13544.

In Situ XANES of SO$_x$ Storage Catalysts

J. Phys. Chem. B, Vol. 109, No. 46, 2005 **21843**

situ studies of the sulfur storage reaction. In contrast, X-ray absorption spectroscopy is frequently used for in situ studies of the chemical nature and the local structure of elements investigated. XANES of sulfur at the K-edge (2473 eV) has been shown to be very sensitive to the oxidation state of the sulfur species present in the sample.[7-9] The difference in the edge position between S^{2-} and S^{6+}, for example, is around 10 eV, which allows a direct and clear distinction between various natures of the sulfur present.[10,11] Furthermore, due to the direct probe of the interaction between the sulfur species and metal cations resulting from the hybridization of the 3p orbitals of sulfur and the 3d orbitals of the metal cations, the technique reveals information about this relationship.[12]

To study the chemical nature of sulfur, however, due to the low energy of the S K absorption edge (2473 eV) advanced experimental setups and specifically designed beam lines are necessary for in situ experiments. This mainly results from the high background absorption at the relative low energy, which requires the minimization of the path length of the X-rays in the gas atmosphere of the reactant gas mixture and the use of a vacuum outside the in situ reaction chamber. We have designed an in situ cell allowing us to monitor the changes in the S K-edge XANES during exposure of the materials to SO$_x$ at elevated temperatures. A similar approach was already published by Hayter et al.; however, the limited temperature range up to 452 K made this approach not applicable for our investigations.[13]

2. Experimental Section

A picture of the XAS cell used for in situ experiments at the sulfur K-edge is shown in Figure 1. The sample is placed inside a reaction chamber sealed against the vacuum with a 7.5 μm Kapton window to measure the fluorescence of the sample exposed to the X-ray beam. The outside of the cell was evacuated to minimize the scattering of the gas phase. Note that in this energy range the 7.5 μm Kapton window leads to an absorption of 25% of the X-ray beam. The sample was heated with a heating wire (thermocoax) around the sample holder controlled by a K-type thermocouple. Special care has to be taken in the design of the sealing, being a crucial part in the experimental setup, by using thermally stable graphite sheets between the metal parts of the cell and the Kapton windows. The samples were inserted as self-supporting wafers. The reactant gas mixtures were controlled by electronic mass flow controllers, using a total flow of 100 mL/min in the reaction chamber. The setup allowed experiments in the temperature range between 273 and 573 K at 1 bar total pressure of the reactants.

The experiments were carried out on the XAFS beam line at the ANKA Angströmquelle Karlsruhe. The storage ring was operated at 2.5 GeV with an electron current between 100 and 200 mA. A double-crystal monochromator equipped with Si(111) crystals was used for the experiments at the S K-edge (2480 eV). Contributions of higher order reflections on the monochromator crystals were minimized by detuning the second crystal to 60% of the maximum intensity. For the experiments at the S K-edge (2480 eV) the (monochromatic) flux rate on the sample was about 2 × 10^{11} photons/s. Harmonic rejection was provided by a grazing incidence premirror which acted as a high-energy filter. All measurements were performed in fluorescence mode using a Si-drift detector (Ketek, Munich, Germany) with an area of 10 mm^2. For energy calibration, the maximum of the first resonance ("white line") in the spectrum of ZnSO$_4$ was set to an energy of 2481.4 eV. For the removal
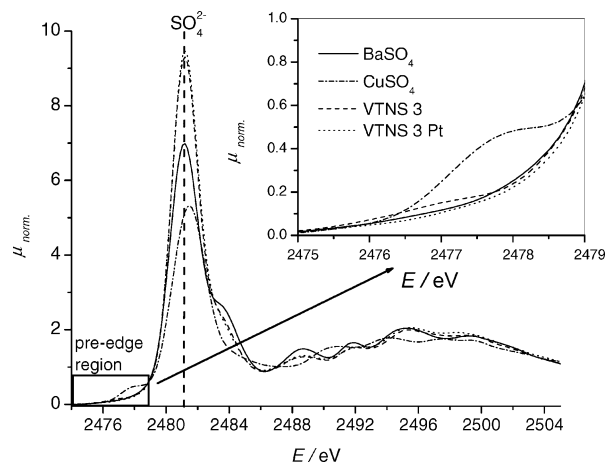

Figure 2. S K-edge spectra of the VTNS 3 (dashed line) + VTNS 3 Pt (dotted line) sample after treatment under dynamic conditions in the plug flow reactor (10 ppm SO$_2$ + 12% O$_2$) and CuSO$_4$ (dashed−dotted line) + BaSO$_4$ (full line) as reference samples.

of scattering contributions and for normalizing the spectra to the amount of material exposed to the X-ray beam a linear background was fitted to the preedge region (2460−2473 eV) and the postedge region (2506−2535 eV) using the software Sixpack V 0.51.[14] A least-squares fitting method was applied using a combination of Gaussian peaks to simulate the contributions of the electron transitions to empty orbitals of the different sulfur species, and an arctangent function was used to model the edge step feature in the XANES corresponding to 1s excitations into continuum states.[15,16] The peak position and fwhm were kept constant over a sample investigated while applying the least-squares fitting procedure. The relative fractions of the sulfur species present on the samples were calculated based on the area of the peaks assigned to sulfite and sulfate species as a function of exposure to oxidizing and reducing conditions.

The SO$_x$ uptake capacities of the material studied at 523 K were determined with a plug flow reaction system described in detail elsewhere.[17] The material investigated was an industrial (second-generation) SO$_x$ trap material containing Ba as the potential SO$_x$ storage component on a CuO−Al$_2$O$_3$ support prepared by Venezia Tecnologia. To study the influence of Pt as an SO$_2$ oxidation component on the SO$_x$ storage process the sample was additionally impregnated with Pt. The samples are named VTNS 3 for the sample without Pt and VTNS 3 Pt for the sample impregnated with Pt.

3. Results and Discussions

The results obtained from various other characterization techniques (BET, XRD, SEM) did not show differences in the structure of the main components (support and storage component) on the sample with and without Pt. The S K-edge spectra of the ex situ prepared samples with and without Pt exposed to lean/rich cycle conditions in the plug flow reactor are compared with those of Ba and Cu sulfate (reference compounds) in Figure 2. The position of the strong peak ("white line") in the spectra at 2480 eV, assigned to the 1s → 3p transition, indicates the presence of S^{6+} (SO$_4^{2-}$) species in all samples.[18] The insert shows the magnification of the preedge region, where an additional preedge peak around 2478 eV was observed on CuSO$_4$, and a very weak feature around 2477 eV was seen on the Pt-free sample. This characteristic preedge peak (2478 eV) at the S K-edge for d elements (e.g., copper sulfate) is assigned to the transition from the S 1s to the ψ^* state formed from the
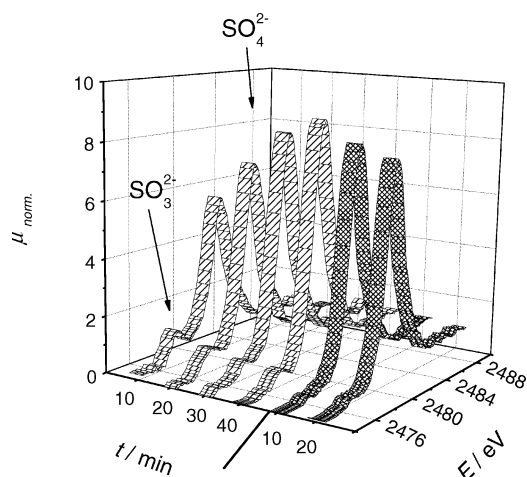
Figure 3. Time-resolved in situ S K-edge spectra of the VTNS 3 Pt at 523 K exposed to 10 ppm SO_2 + 12% O_2 (oxidizing conditions, medium-striped ribbons) and 5% H_2 in He (reducing conditions, dense-striped ribbons).
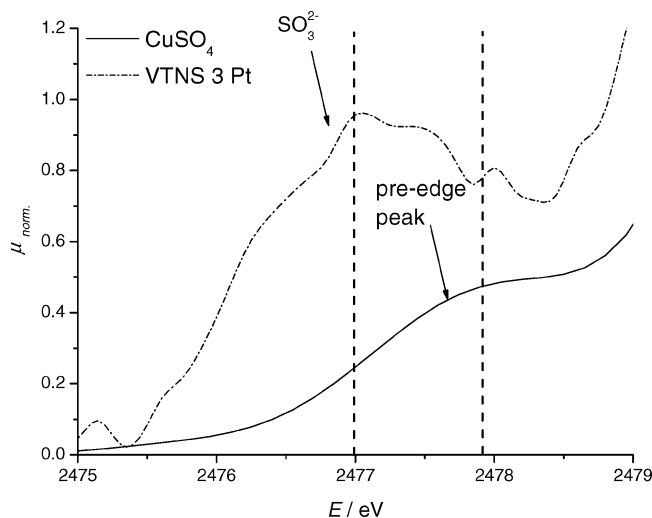

Figure 4. S K-edge spectra of the VTNS 3 Pt (dashed line) at 523 K exposed for 20 min to 10 ppm SO_2 + 12% O_2 (oxidizing conditions) and $CuSO_4$ as reference material.

Figure 5. Time-resolved in situ S K-edge spectra of VTNS 3 without Pt at 523 K exposed to 10 ppm SO_2 + 12% O_2 (oxidizing conditions, medium-striped ribbons) and 5% H_2 in He (reducing conditions, dense-striped ribbons).

Figure 6. S K-edge spectra and least-squares-fitted results of VTNS 3 Pt after 10 min exposure to 10 ppm SO_2 + 12% O_2 at 523 K (full line = original spectra; dashed line = sulfate species; short dotted line = sulfite species; dotted line = arc tan function; dashed−dotted line = summed simulated spectra).

overlap of the S 3p and the metal $3d_{x^2-y^2}$ orbitals in the metal sulfate.[19] If the metal 3d orbitals are half-filled, they contain a significant contribution of the ligand 3p orbital due to their high localization. Therefore, the characteristic shape of the postedge indicates the presence of $BaSO_4$ in the samples. However, applying a least-squares fitting method to distinguish clearly the type of sulfates present on the sample, as previously reported by Dathe et al., was not successful.[20]

The in situ XANES of the Pt-containing SO_x trap material during exposure to SO_2 under oxidative and reductive conditions are shown in Figure 3. During exposure to 10 ppm SO_2 in an oxidative atmosphere a strong peak at 2481 eV and a peak around 2477 eV appeared. The peak at 2481 eV, which increased in intensity with increasing SO_2 exposure, is assigned to sulfate species. The smaller peak around 2477 eV showed the highest intensity at the lowest exposure time and decreased with increasing SO_2 exposure. The peak at 2477 eV is compared with the preedge peak of copper sulfate in Figure 4 and clearly shows a difference in the peak positions (determined using the first derivative of the spectrum) for the SO_2-treated VTNS3 Pt sample as well as the reference $CuSO_4$. The similar position of this peak and the peak maxima of sulfite materials identified by various authors indicate the presence of sulfur in oxidation
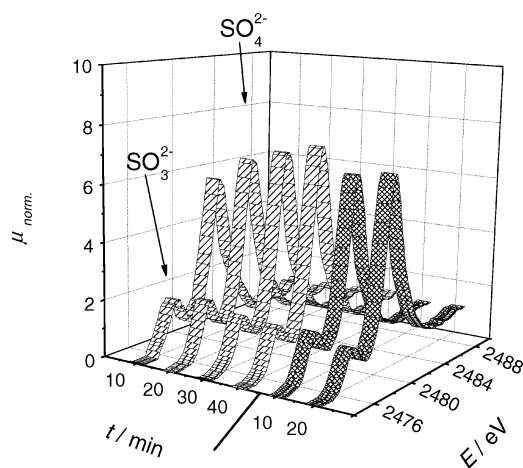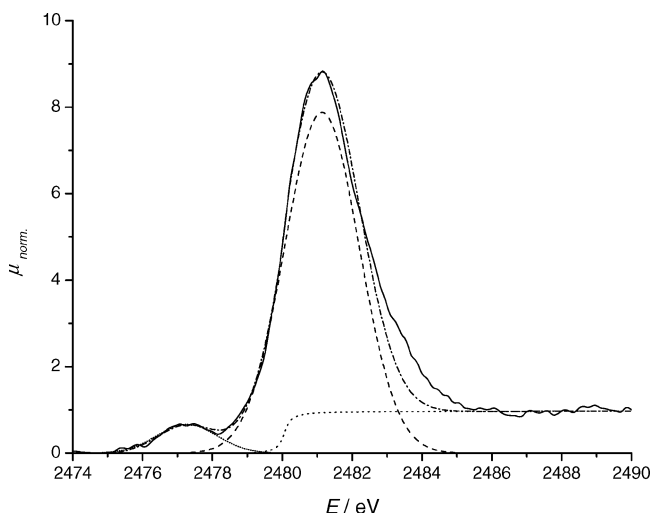
state +4 (attributed to SO_3^{2-}) which was not observed on the ex situ treated sample.[10,11] After switching to a reducing atmosphere (5% H_2 in He) (see Figure 3, dense-striped ribbons) the intensity of both peaks decreases with increasing reduction time. The time-resolved XANES at the S K-edge of the Pt-free sample under these reaction conditions are shown in Figure 5. Under oxidizing conditions two peaks appear in the S K-edge region around 2481 and 2477 eV, i.e., at energies similar to those obtained with the Pt-containing sample. However, with increasing SO_2 exposure the intensity of the peak assigned to the sulfite species remains constant, while the intensity of the peak assigned to sulfate increases. After switching to reducing conditions a slight decrease of both peaks was observed.

As mentioned in the Experimental Section the fraction of sulfite and sulfates were quantified by applying a least-squares fitting procedure. Note that the intensity of the peak assigned to the electron transitions strongly depends on the occupancy of the S p states, and therefore, the intensities of the peak for S^{4+} and S^{6+} cannot directly be compared, as shown by Huffman et al.[15] An example fit for the S K-edge of VTNS 3 Pt after 40 min of exposure to 10 ppm SO_2 + 12% O_2 is shown in Figure 6. The relative fraction of the samples in dependence of the

In Situ XANES of SO$_x$ Storage Catalysts

J. Phys. Chem. B, Vol. 109, No. 46, 2005 **21845**

TABLE 1: Relative Fractions of Sulfate (S^{6+}) and Sulfite (S^{4+}) Present on the Samples at 523 K

	t/min 10 ppm SO$_2$ + 12% O$_2$								t/min 5% H$_2$ in He			
	10		20		30		40		10		20	
material	SO$_3^{2-}$	SO$_4^{2-}$	SO$_3^{2-}$	SO$_4^{2-}$	SO$_3^{2-}$	SO$_4^{2-}$	SO$_3^{2-}$	SO$_4^{2-}$	SO$_3^{2-}$	SO$_4^{2-}$	SO$_3^{2-}$	SO$_4^{2-}$
VTNS 3 Pt	0.16	0.84	0.10	0.90	0.07	0.93	0.05	0.95	0.02	0.98	0.03	0.97
VTNS 3	0.19	0.81	0.17	0.83	0.14	0.86	0.13	0.87	0.15	0.85	0.12	0.88

exposure time is shown in Table 1. After 10 min of exposure to 10 ppm SO$_2$ in 12% O$_2$, 16% of the total sulfur present on the VTNS 3 Pt sample is in the form of sulfite. With increasing exposure the fraction of sulfite decreases, and sulfate species were formed on the Pt-containing sample. After switching to reducing conditions (5% H$_2$ in He) a further decrease of the fraction of sulfite species (from 0.05 to 0.03) was observed. On the Pt-free sample, initially a higher fraction of sulfite species was observed after 10 min under oxidizing conditions compared to that of the Pt-containing material. With increasing exposure time under oxidizing conditions only a slight decrease of the sulfite concentration was observed. After switching to reducing conditions the sulfite concentration seems to be hardly influenced. A comparison of VTNS 3 Pt and VTNS 3 showed that a higher concentration of sulfate species existed in the Pt-containing sample. However, imposing reducing conditions subsequently hardly influenced the fraction of sulfite in the VTNS 3 sample, while on the Pt-containing sample the sulfite species were almost completely removed. Note that in the typical exhaust gas stream CO and hydrocarbons will be additionally present under rich conditions; however, preliminary experiments have shown that these components do not influence the formation of sulfates and sulfites during the SO$_x$ storage process.

Provided that the metal oxide materials for SO$_2$/SO$_3$ storage have the same physicochemical properties, the results indicate that, expectedly, Pt enhances the activity for SO$_2$ oxidation/reduction. Lean/rich cycling experiments under flow conditions (not shown here) showed the formation of SO$_2$ under fuel-rich conditions (240 s lean mode/18 s rich mode) for both materials, with a markedly higher amount of SO$_2$ released from the Pt-containing material. During the typical operation conditions of a NO$_x$ storage−reduction catalyst (i.e., periodic variation between an oxidizing and a reducing atmosphere) the release of SO$_x$ from the SO$_x$ trap observed under reducing conditions will cause deactivation of the NO$_x$ storage catalyst. Therefore, the complete and irreversible SO$_x$ storage is essential for a permanent protection of the catalyst.

The influence of water present in the gas mixture on both materials was investigated under plug flow experiments revealing a strongly enhanced SO$_x$ storage capacity under lean conditions, as well as a reduced SO$_2$ release under reducing conditions. To investigate the influence of water on the nature of the sulfur formed during the SO$_x$ storage process, XANES experiments with 10% H$_2$O in air were carried out in the same manner. Figure 7 depicts the time-resolved in situ S K-edge XANES of the VTNS 3 Pt sample in the presence of water at 523 K. The formation of a peak at 2481.2 eV is observed indicating the formation of sulfates on the material; the formation of sulfuric acid on the material however could not be ruled out. Furthermore, a small contribution appears at 2476.4 eV denoting the presence of sulfite-type species. With respect to the S K-edge XANES under dry conditions (see Figure 3) and the plug flow experiments a supporting effect on the sulfate formation could be assumed, which is most likely caused by the formation of sulfuric acid. It is important to note that at 523 K thermodynamic limitations on the formation of sulfuric acid do not exist. Switching to reducing conditions showed no
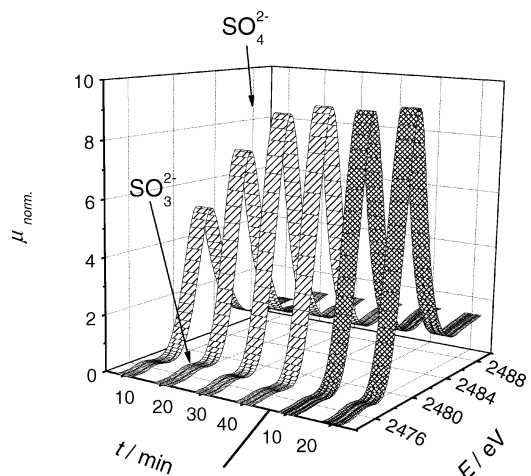

Figure 7. Time-resolved in situ S K-edge spectra of the VTNS 3 Pt at 523 K exposed to 10 ppm SO$_2$ + 12% O$_2$ + 10% H$_2$O (oxidizing conditions, medium-striped ribbons) and 5% H$_2$ in He (reducing conditions, dense-striped ribbons).
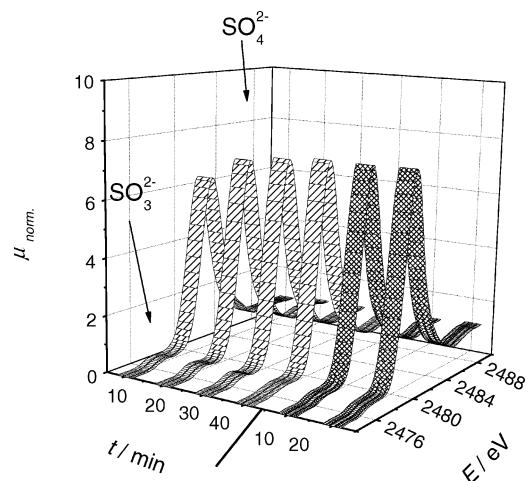

Figure 8. Time-resolved in situ S K-edge spectra of VTNS 3 without Pt at 523 K exposed to 10 ppm SO$_2$ + 12% O$_2$ + 10% H$_2$O (oxidizing conditions, medium-striped ribbons) and 5% H$_2$ in He (reducing conditions, dense-striped ribbons).

strong influence on the nature of the sulfur formed, which could explain the lowered SO$_2$ release under fuel-rich conditions in the presence of water. The S K-edge XANES of the Pt-free sample exposed to the same gas mixture is shown in Figure 8. Clearly one adsorption band at 2481 eV was observed, giving evidence for the formation of sulfates. The small band appearing at 2477 eV proves the existence of sulfite-type species also in the presence of water. Although the intensity of this peak is smaller compared to that of the dry conditions (see Figure 5), the presence of sulfite species explains the higher SO$_2$ storage capacity in the presence of water due to the elimination of a potential rate-limiting oxidation step. The relative fraction of the sulfate and sulfite species formed in dependence of the SO$_2$ exposure time is depicted in Table 2. On both materials the main fraction observed is sulfate with a slightly higher sulfite fraction on the Pt-free sample. Even switching to reducing

TABLE 2: Relative Fractions of Sulfate (S^{6+}) and Sulfite (S^{4+}) Present on the Samples at 523 K

| | *t*/min 10 ppm SO$_2$ + 12% O$_2$ + 10% H$_2$O | | | | | | | | *t*/min 5% H$_2$ in He + 10% H$_2$O | | | |
| | 10 | | 20 | | 30 | | 40 | | 10 | | 20 | |
material	SO$_3^{2-}$	SO$_4^{2-}$	SO$_3^{2-}$	SO$_4^{2-}$	SO$_3^{2-}$	SO$_4^{2-}$	SO$_3^{2-}$	SO$_4^{2-}$	SO$_3^{2-}$	SO$_4^{2-}$	SO$_3^{2-}$	SO$_4^{2}$
VTNS 3 Pt	0.02	0.98	0.02	0.98	0.02	0.98	0.01	0.99	0.01	0.99	0.02	0.98
VTNS 3	0.04	0.96	0.03	0.97	0.03	0.97	0.03	0.97	0.03	0.97	0.03	0.97

conditions only hardly influences the relative fractions of the sulfur species. The obtained results in the presence of water strongly suggest that water facilitates the oxidation of the sulfite species to hardly reducible sulfate species which are stable under fuel-rich conditions leading to a reduced SO$_2$ release under cycling conditions.

4. Conclusions

The results obtained from the in situ S K-edge XANES experiments clearly show that the release of SO$_2$ under rich conditions is caused by the reduction of the sulfite species present. In contrast with the Pt-containing sample, the sulfite species were stable under reducing conditions in absence of Pt, while maintaining a similar total SO$_2$ uptake capacity. Thus, SO$_x$ trapping materials without a noble metal are a clearly better option. Furthermore, the presence of water accelerates the sulfite oxidation leading to a lower relative sulfite fraction observed, probably caused by the production of sulfuric acid. Therefore, the reduced SO$_2$ release under fuel-rich conditions could result from the higher relative fraction of the stable sulfate present. The results shown here demonstrate that monitoring of the oxidation state of sulfur by in situ S K-edge X-ray adsorption spectroscopy leads to a better understanding and shows the key parameters for designing SO$_x$ trapping materials. Rational and rapid development of a new generation of such materials on the basis of complex oxide catalysts that take up SO$_x$ rapidly, but prevent the reduction/release during the lean/reach cycles, using the leads described here is under way.

References and Notes

(1) Kreuzer, T.; Lox, E. S.; Lindner, D.; Leyrer, J. *Catal. Today* **1996**, *29*, 17.

(2) Takeuchi, M.; Matsumoto, S. *Top. Catal.* **2004**, *28*, 151.

(3) Sedlmair, C.; Seshan, K.; Jentys, A.; Lercher, J. A. *Catal. Today* **2002**, *75*, 413.

(4) Fridell, E.; Amberntsson, A.; Olsson, L.; Grant, A. W.; Skoglundh, M. *Top. Catal.* **2004**, *30−31*, 143.

(5) Chigapov, A. N.; Dubkov, A. A.; Carberry, B. P.; Montreuil, C. N.; Graham, G. W.; McCabe, R. W.; Chun, W. *SO$_x$ Trap for Diesel and Lean Burn Gasoline Automotive Applications.* US Patent 1374978 A1 20040102, 2004.

(6) Limousy, L.; Mahzoul, H.; Brilhac, J. F.; Gilot, P.; Garin, F.; Maire, G. *Appl. Catal., B* **2003**, *42*, 237.

(7) Solomon, D.; Lehmann, J.; Martinez, C. E. *Soil Sci. Soc. Am. J.* **2003**, *67*, 1721.

(8) Najman, M. N.; Kasrai, M.; Bancroft, G. M. *Wear* **2004**, *257*, 32.

(9) George, G. N.; Gorbaty, M. L. *J. Am. Chem. Soc.* **1989**, *111*, 3182.

(10) Vairavamurthy, A. *Spectrochim. Acta, Part A* **1998**, *54*, 2009.

(11) Myneni, S. C. B. *Rev. Mineral. Geochem.* **2000**, *40*, 113.

(12) Williams, K. R.; Hedman, B.; Hodgson, K. O.; Solomon, E. I. *Inorg. Chim. Acta* **1997**, *263*, 315.

(13) Hayter, C. E.; Evans, J.; Corker, J. M.; Oldman, R. J.; Williams, B. P. *J. Mater. Chem.* **2002**, *12*, 3172.

(14) Webb, S. *SixPack.* 0.51 ed.; Stanford Synchrotron Radiation Laboratory: Menlo Park, CA, 2004.

(15) Huffman, G. P.; Mitra, S.; Huggins, F. E.; Shah, N.; Vaidya, S.; Lu, F. L. *Energy Fuels* **1991**, *5*, 574.

(16) Waldo, G. S.; Carlson, R. M. K.; Moldowan, J. M.; Peters, K. E.; Pennerhahn, J. E. *Geochim. Cosmochim. Acta* **1991**, *55*, 801.

(17) Dathe, H.; Peringer, E.; Roberts, V.; Jentys, A.; Lercher, J. A. *C. R. Chim.* **2005**, *8*, 753.

(18) Li, D.; Bancroft, G. M.; Kasrai, M.; Fleet, M. E.; Feng, X. H.; Tan, K. *Can. Mineral.* **1995**, *33*, 949.

(19) Szilagyi, R. K.; Frank, P.; George, S. D.; Hedman, B.; Hodgson, K. O. *Inorg. Chem.* **2004**, *43*, 8318.

(20) Dathe, H.; Jentys, A.; Lercher, J. A. *Phys. Chem. Chem. Phys.* **2005**, *7*, 1283.